# On the calculation of rotational anisotropy decay, as measured by ultrafast polarization-resolved vibrational pump-probe experiments

Y.-S. Lin, P. A. Pieniazek, Mino Yang, and J. L. Skinner

Citation: J. Chem. Phys. **132**, 174505 (2010); doi: 10.1063/1.3409561
View online: https://doi.org/10.1063/1.3409561
View Table of Contents: http://aip.scitation.org/toc/jcp/132/17
Published by the American Institute of Physics

# On the calculation of rotational anisotropy decay, as measured by ultrafast polarization-resolved vibrational pump-probe experiments

Y.-S. Lin,[1] P. A. Pieniazek,[1] Mino Yang,[1,2] and J. L. Skinner[1,a)]
[1]*Department of Chemistry and Theoretical Chemistry Institute, University of Wisconsin, Madison, Wisconsin 53706, USA*
[2]*Department of Chemistry, Chungbuk National University, Cheongju, Chungbuk 361-763, Republic of Korea*

(Received 24 February 2010; accepted 5 April 2010; published online 7 May 2010)

Polarization-resolved vibrational pump-probe experiments are useful for measuring the dynamics of molecular reorientation. The rotational anisotropy observable is usually modeled by the second-Legendre-polynomial time-correlation function of the appropriate molecule-fixed unit vector. On the other hand, more elaborate calculations that include non-Condon effects, excited-state absorption, and spectral diffusion, can be performed using the infrastructure of the nonlinear response formalism. In this paper we present "exact" (within the impulsive limit) results from the nonlinear response formalism, and also a series of approximations that ultimately recover the traditional result mentioned above. To ascertain the importance of these effects not included in the traditional approach, we consider the specific case of dilute HOD in $H_2O$. We find that for the frequency-integrated anisotropy decay, it is important to include non-Condon effects. For the frequency-resolved anisotropy decay, non-Condon effects, excited-state absorption, and spectral diffusion are all important. We compare our results with recent experiments. © *2010 American Institute of Physics*. [doi:10.1063/1.3409561]

## I. INTRODUCTION

For many years, different types of spectroscopy, such as NMR, dielectric relaxation, terahertz, optical Kerr effect, and quasielastic neutron scattering, have been used to probe molecular dynamics in condensed phases.[1–14] More recently, ultrafast vibrational pump-probe experiments have proven to be very useful for studying rotational dynamics. Consider a vibrational mode on a molecule in a condensed phase, in the case that the vibrational transition of this mode is spectrally and/or physically isolated from other modes in the system. The unit vector of the transition dipole for this vibration reorients in time as the molecule rotates and undergoes possible conformational dynamics. The reorientation dynamics of this unit vector can be measured by polarization-resolved pump-probe experiments, as follows. A linearly polarized pump beam, resonant with the vibrational transition, is incident on the sample, and then the transient absorption is measured with a time-delayed resonant probe beam, polarized either parallel or perpendicular to the pump beam. The rotational anisotropy decay is constructed by[4,15–18]

$$r(t) \equiv \frac{S^{\|}(t) - S^{\perp}(t)}{S^{\|}(t) + 2S^{\perp}(t)}, \tag{1}$$

where $S^{\|}(t)$ is the absorption change when the probe is parallel to the pump, $S^{\perp}(t)$ is the absorption change when the probe is perpendicular to the pump, and $t$ is the time delay between pump and probe.

The spectral widths of vibrational transitions can be substantial, and so important additional variables are the frequencies of the pump and probe beams. A theoretical treatment of pump-probe experiments with narrow-band radiation involves convolutions over the pulse envelopes. In a common variant used recently, however, the pump and probe beams are sufficiently short that the bandwidth of the pulses covers the vibrational transition.[17,19,20] Thus, the pump pulse excites the full ensemble of vibrations, and in the "frequency-integrated" experiment the total transient absorption (integrated over all frequencies) is measured. On the other hand, one can also measure the "frequency-resolved" signal, by passing the transmitted beam through a monochrometer.[17,19,20] These "impulsive" experiments are easier to deal with theoretically.

Polarization-resolved pump-probe experiments are usually interpreted by assuming that the anisotropy decay is given by the rotational time-correlation function[15–18,21–23]

$$r(t) = \frac{2}{5}\langle P_2(\hat{u}(0)\cdot\hat{u}(t))\rangle, \tag{2}$$

where $P_2(x)$ is the second Legendre polynomial, $\hat{u}(t)$ is the time-dependent unit vector of the transition dipole, and the angular brackets indicate an equilibrium ensemble average. Actual derivations of this result for vibrational pump-probe spectroscopy seem to be absent; one usually invokes derivations appropriate for NMR experiments.[24] For the frequency-resolved signal discussed above, the anisotropy decay has been calculated with Eq. (2), but including only those molecules whose vibration is in a narrow frequency window at time $t$ (or equivalently, at time 0).[19,25] For one-color narrow-band experiments, a similar result, but where the frequency is in a narrow frequency window at 0 *and* $t$, has also been employed.[26]

a)Electronic mail: skinner@chem.wisc.edu.

 

On the other hand, one can calculate the anisotropy decay using the full infrastructure of nonlinear response functions.[5] This formalism shows that the signal includes contributions from the "ground-state bleach" (the pump pulse depletes the ground-state, $v=0$, population), "stimulated emission" (molecules excited by the pump to $v=1$ are stimulated to emit by the probe), and "excited-state absorption" (molecules excited by the pump to $v=1$ can be further excited to $v=2$ by the probe).[5,27,28] Moreover, the nonlinear response function formalism includes non-Condon effects (where the magnitude of the transition dipole depends on the molecular environment of the vibrational chromophore).[29] For the frequency-resolved experiments, the nonlinear response formalism takes into account spectral diffusion (time-dependent fluctuations of the vibrational transition frequency).[30] None of the consequences of excited-state absorption, non-Condon effects, and spectral diffusion are included in the simple formula Eq. (2), or its frequency-dependent generalization. Indeed, since Eq. (2) has not been derived from the nonlinear response formalism, it is not clear under what conditions it should be valid.

One final point involves the vibrational excited state lifetime. This is usually taken to be a constant, independent of molecular environment, in which case lifetime effects cancel out in (the numerator and denominator of) Eq. (1). On the other hand, it is now being appreciated that, especially for heterogeneous situations such as solutions[31–33] or interfaces,[18,34–38] but even possibly for homogeneous solutions,[39] vibrational lifetimes can depend strongly on molecular environment. These effects can be included within the nonlinear response formalism, but, again, they are not present in Eq. (2). This point has been discussed recently by Fayer and co-workers[32,33,36–38] and by Laage and Hynes.[40]

The goals of this paper are threefold. First, starting with the nonlinear response formalism, we derive expressions for the anisotropy decay within various approximations, showing under what conditions one recovers Eq. (2). Second, for a specific example, dilute HOD in $H_2O$, we demonstrate the effects of including the various contributions discussed above. We find that for the frequency-integrated signal, it is important to include non-Condon effects. For the frequency-resolved signal, non-Condon effects, excited-state absorption, and spectral diffusion *all* increase the anisotropy. Third, we compare our new and more correct (within the model) results with recent experiments.[19,20]

## II. PUMP-PROBE ANISOTROPY DECAY

In order to compute the anisotropy decay measured by ultrafast infrared (IR) pump-probe spectroscopy, one starts from the third-order response functions.[5] In general there are three incident laser pulses, with wave vectors $\vec{k}_1$, $\vec{k}_2$, and $\vec{k}_3$, and electric field polarizations in the directions $\hat{i}$, $\hat{j}$, and $\hat{k}$, respectively. The field amplitude is detected with polarization $\hat{l}$. The time delay between the first and second pulses is $t_1$, that between the second and third is $t_2$, and that between the third pulse and detection is $t_3$. For an isolated chromophore within the mixed quantum/classical approximation, and for the moment neglecting lifetime processes, the eight response functions, $R_n^{ijkl}(t_1,t_2,t_3)$, are given in Appendix A.

Herein, we will consider pump-probe experiments in the impulsive (infinitely short pulse) limit. Moreover, in pump-probe experiments $\vec{k}_1=\vec{k}_2$ and $t_1=0$ (since the first and second interactions come from the same laser pulse), and the signal is observed in the $\vec{k}_3$ direction, and so $R_7$ and $R_8$ do not contribute. Finally, the sums of the rephasing $(R_1+R_2+R_3)$ and nonrephasing $(R_4+R_5+R_6)$ terms are identical, and in addition, $i=j$ and $k=l$. Therefore, under these circumstances, the total response function is simply

$$R^{iikk}(0,t_2,t_3) \sim 2R_1^{iikk}(0,t_2,t_3) + R_3^{iikk}(0,t_2,t_3). \tag{3}$$

### A. Frequency-resolved and frequency-integrated pump-probe signals

For the frequency-resolved signal[5,41]

$$S^{iikk}(t_2,\omega_3) = Re\left[\int_0^\infty dt_3 e^{i\omega_3 t_3} R^{iikk}(0,t_2,t_3)\right] \tag{4}$$

and so the measured anisotropy decay, from Eq. (1), is

$$r(t_2,\omega_3) \equiv \frac{S^{iiii}(t_2,\omega_3) - S^{iikk}(t_2,\omega_3)}{S^{iiii}(t_2,\omega_3) + 2S^{iikk}(t_2,\omega_3)}. \tag{5}$$

In this equation, $\hat{i}\perp\hat{k}$.

For the frequency-integrated signal, one integrates $S^{iikk}(t_2,\omega_3)$ over $\omega_3$, which gives

$$S^{iikk}(t_2) \sim R^{iikk}(0,t_2,0) \sim 2\langle \mu_{10}^i(0)^2 \mu_{10}^k(t_2)^2\rangle - \langle \mu_{10}^i(0)^2 \mu_{21}^k(t_2)^2\rangle \tag{6}$$

so then the anisotropy decay becomes

$$r(t_2) = \frac{R^{iiii}(0,t_2,0) - R^{iikk}(0,t_2,0)}{R^{iiii}(0,t_2,0) + 2R^{iikk}(0,t_2,0)}, \tag{7}$$

where, again, $\hat{i}\perp\hat{k}$.

### B. Approximate frequency-integrated signals

If one makes the reasonable assumption that $\vec{\mu}_{21}(t) \propto \vec{\mu}_{10}(t)$, then Eq. (7) simplifies considerably to

$$r(t_2) = \frac{\langle \mu_{10}^i(0)^2 \mu_{10}^i(t_2)^2\rangle - \langle \mu_{10}^i(0)^2 \mu_{10}^k(t_2)^2\rangle}{\langle \mu_{10}^i(0)^2 \mu_{10}^i(t_2)^2\rangle + 2\langle \mu_{10}^i(0)^2 \mu_{10}^k(t_2)^2\rangle} \tag{8}$$

except in the harmonic limit, for which $\vec{\mu}_{21}(t)=\sqrt{2}\vec{\mu}_{10}(t)$, and the signal is identically zero. Note that the result of Eq. (8) is also obtained if one simply makes the "two-level" approximation (neglecting the excited-state absorption contribution from the 2–1 transition). In Appendix B we show that the above result is equal to

$$r(t_2) = \frac{1}{5}\left(3\frac{\langle(\vec{\mu}_{10}(0)\cdot\vec{\mu}_{10}(t_2))^2\rangle}{\langle|\vec{\mu}_{10}(0)|^2|\vec{\mu}_{10}(t_2)|^2\rangle} - 1\right). \tag{9}$$

The transition dipole can be written as

$$\vec{\mu}_{10}(t) = \mu_{10}(t)\hat{u}(t), \tag{10}$$

where $\mu_{10}(t)$ is its magnitude, and $\hat{u}(t)$ is the unit vector. Within the Condon approximation, $\mu_{10}(t)$ is constant, and so Eq. (9) becomes

$$r(t_2) = \frac{2}{5}\langle P_2(\hat{u}(0)\cdot\hat{u}(t_2))\rangle, \tag{11}$$

as in Eq. (2). Note that this result is also obtained if the dynamics of the magnitude of the transition dipole and its direction are statistically uncorrelated

$$\langle \mu_{10}(0)^2\mu_{10}(t)^2(\hat{u}(0)\cdot\hat{u}(t))^2\rangle = \langle \mu_{10}(0)^2\mu_{10}(t)^2\rangle\langle(\hat{u}(0)\cdot\hat{u}(t))^2\rangle. \tag{12}$$

We can now summarize the conditions for the validity of Eq. (2): impulsive excitation, frequency-integrated detection, $\vec{\mu}_{21}(t)\propto\vec{\mu}_{10}(t)$ or the two-level approximation, and Condon approximation or factorization approximation as described above.

### C. Approximate frequency-resolved signals

In this case, one can make a series of approximations starting with Eqs. (3)–(5). For example, within the two-level approximation one simply drops the excited-state absorption ($R_3$) term in Eq. (3), so

$$R^{iikk}(0,t_2,t_3) \sim R_1^{iikk}(0,t_2,t_3), \tag{13}$$

and proceeds using Eqs. (4) and (5).

One can, in addition, make the Condon approximation, so that

$$R^{iikk}(0,t_2,t_3) \sim \langle u^i(0)^2u^k(t_2)u^k(t_2+t_3)e^{-i\int_{t_2}^{t_2+t_3}d\tau\omega_{10}(\tau)}\rangle, \tag{14}$$

where $u^i$ is the $i$th component of the unit vector $\hat{u}$.

To proceed further it is necessary to make the approximation that the $k$th component of the transition dipole unit vector does not change during the dephasing period $t_3$, so that

$$R^{iikk}(0,t_2,t_3) \sim \langle u^i(0)^2u^k(t_2)^2e^{-i\int_{t_2}^{t_2+t_3}d\tau\omega_{10}(\tau)}\rangle. \tag{15}$$

One can then follow through with the derivation in Appendix B, and we find that

$$r(t_2,\omega_3) = \frac{2}{5}\frac{\langle P_2(\hat{u}(0)\cdot\hat{u}(t_2))Re\int_0^\infty dt_3 e^{i\omega_3t_3}e^{-i\int_{t_2}^{t_2+t_3}d\tau\omega_{10}(\tau)}\rangle}{\langle Re\int_0^\infty dt_3 e^{i\omega_3t_3}e^{-i\int_{t_2}^{t_2+t_3}d\tau\omega_{10}(\tau)}\rangle}. \tag{16}$$

At this point we can consider the "inhomogeneous limit" (where the spectral diffusion dynamics is sufficiently slow that there is no motional narrowing in the line shape).[30,42–45] In this case

$$e^{-i\int_{t_2}^{t_2+t_3}d\tau\omega_{10}(\tau)} \simeq e^{-i\omega_{10}(t_2)t_3}. \tag{17}$$

Within the two-level and Condon approximations, then

$$r(t_2,\omega_3) = \frac{2}{5}\frac{\langle P_2(\hat{u}(0)\cdot\hat{u}(t_2))\delta(\omega_3-\omega_{10}(t_2))\rangle}{\langle\delta(\omega_3-\omega_{10})\rangle}, \tag{18}$$

and since the system is at equilibrium and trajectories are reversible, this is identical to

$$r(t_2,\omega_3) = \frac{2}{5}\frac{\langle P_2(\hat{u}(0)\cdot\hat{u}(t_2))\delta(\omega_3-\omega_{10}(0))\rangle}{\langle\delta(\omega_3-\omega_{10})\rangle}, \tag{19}$$

which is the result that we discussed in Sec. I, involving a narrow frequency window, and which has been used before to calculate frequency-resolved anisotropy decays.[19,25]

Note that if the transition frequency $\omega_{10}$ and rotational dynamics were uncorrelated, then Eq. (19) would reduce to Eq. (11), and there would be no frequency dependence.

### D. Heterogeneous lifetime effects

As discussed in Sec. I, the vibrational lifetime is usually assumed to be constant. Thus, for example, for the frequency-integrated signal within the Condon and two-level approximations, one should multiply both numerator and denominator of Eq. (8) by $e^{-t_2/T_1}$ ($T_1$ is the vibrational lifetime), which then immediately cancels out. This provides the usual understanding that the anisotropy decay is independent of the lifetime. But what if the lifetime is not constant, but rather depends on molecular environment, and hence fluctuates as these environments change in time? In this case, the excited-state population $P_1(t)$ evolves for a particular realization according to

$$\dot{P}_1(t) = -\frac{1}{T_1(t)}P_1(t), \tag{20}$$

which is integrated to give

$$P_1(t)/P_1(0) = e^{-\int_0^t d\tau T_1(\tau)^{-1}}. \tag{21}$$

This factor must now multiply numerator and denominator of Eq. (8), *inside* the averages. Again following through the derivation of Appendix B, within the Condon approximation, we find, for the frequency-integrated anisotropy decay, that

$$r(t_2) = \frac{2}{5}\frac{\langle P_2(\hat{u}(0)\cdot\hat{u}(t_2))e^{-\int_0^{t_2}d\tau T_1(\tau)^{-1}}\rangle}{\langle e^{-\int_0^{t_2}d\tau T_1(\tau)^{-1}}\rangle}. \tag{22}$$

For the special case that $T_1$ can take only two discrete values, this result has been derived and discussed earlier by Laage and Hynes.[40]

## III. RESULTS AND DISCUSSION FOR WATER

The goal of this section is to calculate the anisotropy decay, as measured by vibrational pump-probe experiments, for a specific problem—dilute HOD in $H_2O$—to ascertain the importance of non-Condon effects, spectral diffusion, and excited-state absorption. In other words, are the commonly used approximations of Eqs. (11) and (19) for the frequency-integrated and frequency-resolved anisotropy decay, respectively, valid? We choose to study water because we believe we have reasonably realistic models for calculating spectroscopy observables,[46] and because there have been several recent experiments on this system.[17,19,20]

TABLE I. Relationships for the transition frequencies $\omega_{10}$, $\omega_{21}$ (in $cm^{-1}$), dipole derivative $\mu'$, and 1–0 and 2–1 matrix elements of the OD stretching coordinate $x_{10}$ and $x_{21}$ (in Å). $E$ is the electric field (in a.u.) on the D atom projected along the OD bond. The dipole derivative in the gas phase, $\mu'_g$, is 0.187 49 a.u.

| |
|---|
| $\omega_{10}=2762.6-3640.8E-56\ 641E^2$ |
| $\omega_{21}=2695.8-3785.1E-73\ 074E^2$ |
| $x_{10}=0.0880-1.105\times10^{-5}\omega_{10}$ |
| $x_{21}=0.1229-1.525\times10^{-5}\omega_{21}$ |
| $\mu'/\mu'_g=0.711\ 16+75.591E$ |

### A. Electronic-structure/molecular-dynamics method

For the system under study the vibrational chromophore is the OD stretch, and to calculate the response function one needs to compute, for this mode, $\omega_{10}(t)$, $\omega_{21}(t)$, $\mu_{10}(t)$, $\mu_{21}(t)$, and $\hat{u}(t)$. The latter is taken to be the OD bond unit vector, which can easily be obtained from a molecular dynamics (MD) simulation. The first four quantities can also be obtained from the same MD simulation, provided we have a way of determining them for a given configuration.[25,47–57] In the electronic-structure/molecular-dynamics (ES/MD) method, relationships for the spectroscopic quantities are established from ES calculations on representative clusters, and then used in a MD simulation.[52–54,58–61] Recently, we have reported relationships for the OD stretch of dilute HOD in liquid $H_2O$; thus, the spectroscopic variables can be easily calculated knowing $E$, the electric field on the D atom projected along the OD bond.[22] These relationships are given in Table I (the maps for the 2–1 transition are presented here for the first time). Note that in these relationships the magnitudes of the transition dipoles are written as[29,53]

$$\mu_{10} = \mu' x_{10}, \tag{23}$$

$$\mu_{21} = \mu' x_{21}, \tag{24}$$

where $x_{ij}$ are the matrix elements of the OD stretch vibrational coordinate, and $\mu'$ is the dipole derivative.

A 10 ns MD simulation of 256 simple-point-charge/extended (SPC/E) water molecules[62] was performed using the GROMACS simulation package.[63–67] The Berendsen thermostat was used with a reference temperature of 298.15 K and a coupling time constant of 0.3 ps (we have verified that the results are identical to those for a longer coupling time constant of 1 ps), after equilibration at a reference temperature of 298.15 K with a time constant of 0.01 ps for 200 ps. The simulation time step is 1 fs and the SETTLE algorithm is implemented to constrain the water geometry. The cutoff for the Lennard-Jones interactions is 9 Å, while particle-mesh Ewald was used to calculate the long-range Coulomb interactions.

### B. Frequency-integrated anisotropy decay

We calculate the frequency-integrated rotational anisotropy for three different levels of approximation: (1) three-level system with non-Condon effects ["exact" result, from Eq. (7)], (2) two-level approximation with non-Condon effects [Eq. (9)], (3) traditional "P2" result [with Condon approximation, from Eq. (11)]. Note, of course, that exact means exact within the model of SPC/E water, our spectroscopic maps, third-order response functions, etc. In Fig. 1 we plot the P2 result, and the two-level approximation with non-Condon effects (2L, non-Condon). These results differ only in that the latter includes non-Condon effects. One sees that including these effects makes a substantial difference in the results. The exact results, including the excited-state absorption contribution, are indistinguishable from the two-level approximation with non-Condon effects, and so they are not presented in the figure. This is not surprising, since $\vec{\mu}_{21}(t)$ is almost proportional to $\vec{\mu}_{10}(t)$ (because the electric field dependences of $x_{21}$ and $x_{10}$ are much weaker than that of $\mu'$), which is the condition for the validity of Eq. (9).

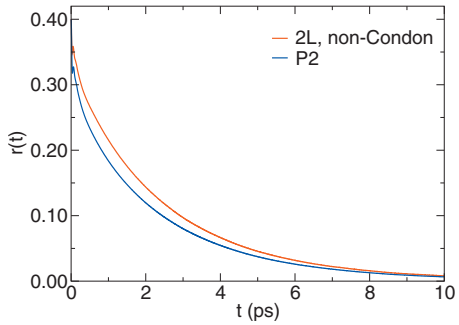


FIG. 1. Theoretical frequency-integrated anisotropy decay, for dilute HOD in $H_2O$. The exact results, from Eq. (7), are indistinguishable from the curve labeled 2L, non-Condon.

The breakdown of the Condon approximation result, Eq. (11), comes about since, in general, OH groups with stronger hydrogen bonds have slower rotational dynamics, and larger transition dipole moments; therefore, including non-Condon effects emphasizes these slower contributions. From a mathematical perspective, this breakdown shows that the factorization in Eq. (12) is not satisfied. Indeed, since larger transition dipole magnitudes and slower rotational dynamics are positively correlated, the left-hand side of Eq. (12) is greater than the right-hand side, and so the anisotropy in Eq. (9) is larger than that in Eq. (11).

### C. Frequency-resolved anisotropy decay

In this case we also present a series of different approximations: (1) three-level system with non-Condon effects [exact result from Eqs. (3)–(5)], (2) two-level approximation with non-Condon effects [from Eqs. (13), (4), and (5)], (3) two-level and Condon approximations [from Eq. (14)], (4) P2 result [including two-level, Condon, and inhomogeneous approximations, from Eq. (19)]. We show the results for a probe frequency near the middle of the band (2520 $cm^{-1}$) in Fig. 2.

Starting with the most severe P2 approximation, shown by the blue line, we first note that this is larger or smaller than the frequency-integrated P2 result shown in Fig. 1, if the frequency is on the red or the blue side of the line, respectively. This is because molecules on the blue side, with weak or broken hydrogen bonds, have rotational dynamics faster than average, while those on the red side have rotational dynamics slower than average. For this particular

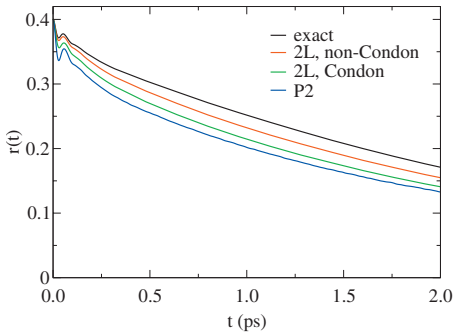


FIG. 2. Theoretical frequency-resolved anisotropy decay, with a probe frequency of 2520 $cm^{-1}$.

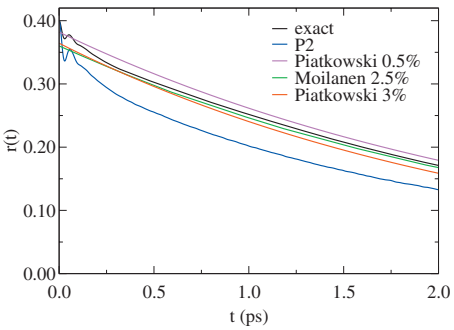


FIG. 3. Theoretical and experimental (Refs. 19 and 20) frequency-resolved anisotropy decay, at a probe frequency of 2519 or 2520 $cm^{-1}$.

probe frequency near the middle of the band the frequency-resolved anisotropy decay in Fig. 2 is slightly larger than the frequency-integrated anisotropy decay shown in Fig. 1.

We now compare the P2 approximation with the "2L, Condon" result (green line). The main difference between these two results is the neglect of spectral dynamics during the $t_3$ period in the former. This comparison shows that the effects of spectral diffusion are quantitatively important. In particular, we see that spectral diffusion increases the anisotropy. This is because slow spectral dynamics are positively correlated with slow rotational dynamics. Slow spectral dynamics leads to a larger contribution to the half-Fourier transform in Eq. (16), and this positive correlation leads to a larger anisotropy than in Eq. (19).

We next consider the 2L, non-Condon curve (red line). The only difference between 2L, Condon and this is the Condon approximation in the former. As in the previous section, we find that making this approximation produces significant errors, and as before, the results with non-Condon effects are substantially larger, for all times. Finally, we compare to the exact result. From this we see that making the two-level approximation leads to substantial error. This is in contrast to what we found for the frequency-integrated decay (where the two-level approximation was excellent). The difference here arises from the spectral shift of the 2–1 transition due to anharmonicity, the correspondingly dissimilar spectral diffusion dynamics of the 2–1 and 1–0 transitions, and the different sign of the response function for the 2–1 transition.

Although the values of the anisotropy shown in Fig. 2 depend on the level of approximation, they all show exponential decay at longer times. And interestingly enough, the values of the decay times are similar, ranging from 2.5 to 2.6 ps for the different approximations (when fit from 1 to 3 ps).

### D. Comparison with experiment

Two ultrafast frequency-resolved IR pump-probe studies on HOD in $H_2O$ have very recently appeared in the literature.[19,20] Both of these studies used 70 fs pulses (which is presumably close enough to the impulsive limit used herein to permit quantitative comparison between theory and experiment), and both groups frequency dispersed the probe beam using an array detector. The earlier result,[19] from a solution of 2.5% $D_2O$ in $H_2O$, for the anisotropy at a frequency of 2519 $cm^{-1}$, is shown in Fig. 3. Actually, what is shown is an exponential fit to the experimental data, which begins at 200 fs (due to pulse overlap and coherent artifact effects). Thus, the portion from 0 to 200 fs is an extrapolation. The more recent study[20] involved a careful investigation of the $D_2O$ concentration dependence. Exponential fits to results for two concentrations, 0.5% and 3%, with a probe frequency averaged from 2480 to 2560 $cm^{-1}$ (thus, nominally at 2520 $cm^{-1}$),[68] are also shown in the figure. As in the previous case, the short-time component of these results should be considered an extrapolation. These experimental results are all consistent with a weak concentration dependence (over this concentration range), showing that higher concentration leads to lower anisotropy, due to residual effects of energy transfer among OD groups.[20]

In the same figure we show our exact frequency-resolved theoretical result, at a probe frequency of 2520 $cm^{-1}$, together with the result from the P2 approximation. One sees that agreement between theory and experiment is significantly improved by the exact calculation. Note, however, that our theoretical calculations are at infinite dilution, and so the results should, in principle, be equal to or larger than the lowest concentration (0.5%) experimental results (which they are not). Note, also, that the theoretical results do not extrapolate exponentially to $t=0$, but rather show interesting structure from 0 to 250 fs, due to molecular libration.[17,19,46]

The study of Moilanen *et al.*[19] also focused on the frequency dependence of the (extrapolated) anisotropy decay at 100 fs, interpreting this drop as resulting from exploration of the librational cone. Their analysis showed that by 100 fs the anisotropy has lost between 10% and 20% of its amplitude, and this drop is an increasing function of the probe frequency. This is reasonable, since a higher frequency indicates a weaker hydrogen bond, allowing more freedom for the molecule to reorient.[19] Experiments were compared with results from simulation, using the P2 approximation in Eq. (19).[19] In Fig. 4 we reproduce these theoretical and experimental results. We also include (extrapolated) experimental points, as a function of probe frequency, for the two concentrations studied by Piatkowski *et al.*[68] We see that their results for the 3% solution are in good agreement with the results of Moilanen *et al.*[19] at a similar concentration (2.5%), while their results for the 0.5% solution are somewhat higher. This implies that a contribution to the initial drop reported by Moilanen *et al.*[19] is actually due to resonant energy transfer.[20]

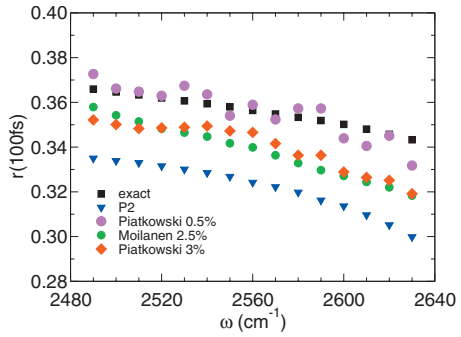


FIG. 4. Theoretical and experimental (Refs. 19, 20, and 68) frequency-resolved anisotropy decay, at 100 fs, as function of probe frequency.

In Fig. 4 we also report the values of the anisotropy decays at 100 fs using our exact theoretical result (full three-level response functions with non-Condon effects included). As anticipated from the above, the exact theoretical results are significantly higher than the P2 results, at all frequencies, because the latter neglect excited-state absorption, non-Condon effects, and spectral diffusion. These exact results, appropriate for infinite dilution, are in quite good agreement with the new experimental results of Piatkowski *et al.*[68] at their lowest concentration of 0.5%. However, one should consider this agreement between theory and experiment warily, since the experimental data come from extrapolations back to 100 fs, while the theoretical results are not extrapolated (and the theoretical result in Fig. 3 shows that such an extrapolation would be misleading).

## IV. CONCLUSION

Starting with the nonlinear response formalism, we have calculated polarization-resolved rotational anisotropy decays, for both the frequency-integrated and frequency-resolved signals. Our exact (within the impulsive limit) results include contributions from non-Condon effects, excited-state absorption, and spectral diffusion. We also present a series of approximate results, as we neglect excited-state absorption, make the Condon approximation, and neglect spectral diffusion. Indeed, in the simplest approximation we recover the standard results involving the second Legendre polynomial.

The question, then, is how valid are these standard results? We illustrate this by considering a specific problem, the rotational dynamics of dilute HOD in $H_2O$. For the frequency-integrated signal we find that it is important to include non-Condon effects. For the frequency-resolved signal, spectral diffusion, non-Condon effects, and excited-state absorption all increase the anisotropy, resulting in curves that are significantly higher than the standard approximation.

We compare our results with experiment[19,20] (on HOD in $H_2O$) for the frequency-resolved anisotropy decay, obtaining good agreement. We also focus on the initial anisotropy drop at short times (100 fs), as a function of frequency. Our previous calculations[19] using the standard results showed the right trend with frequency but were in fact too low (compared to experiment) at all frequencies. Our new results reported herein are now too high compared with the experiment at 2.5% $D_2O$,[19] but in good agreement with new data at 0.5%,[20,68] where the residual effects of OD vibrational energy transfer are minimized. However, this comparison between theory and experiment at 100 fs should be viewed with caution, as the experimental results are extrapolated, while the theoretical results are not.

It is difficult to know if the corrections discussed herein are generally important. Certainly non-Condon effects are more significant for water than for many other systems. On the other hand, the effects of excited-state absorption and spectral diffusion may be more important for other systems. In any case, the work in this paper shows under what circumstances the standard results are valid, and should alert workers to their possible limitations.

One final point: Our theoretical results are valid for electronic spectroscopy as well, simply by making the two-level approximation. Thus, our cautions about non-Condon effects and spectral diffusion may also be appropriate here.

## ACKNOWLEDGMENTS

The authors are indebted to L. Piatkowski and H. J. Bakker for providing the unpublished data shown in Fig. 4. We thank J. R. Schmidt, H. J. Bakker, and L. Piatkowski for helpful discussions, and M. D. Fayer and H. J. Bakker for critical readings of the manuscript. This research was supported by NSF, through Grant No. CHE-0750307, and DOE through Grant No. DE-FG02-09ER16110. M.Y. acknowledges the financial support by the Korean Research Foundation Grant funded by the Korean Government (MOEHRD, Basic Research Promotion Fund) (Grant No. KRF-2008-314-C00166) and the University of Wisconsin Foundation.

## APPENDIX A: NONLINEAR RESPONSE FUNCTIONS

The eight nonlinear response functions, which have signals with the wave vectors as indicated, are

$\vec{k} = -\vec{k}_1 + \vec{k}_2 + \vec{k}_3$:

$$R_1^{ijkl}(t_1,t_2,t_3) = \langle X_1^{ijkl}(t_1,t_2,t_3) e^{i\int_0^{t_1} d\tau \omega_{10}(\tau)} e^{-i\int_{t_1}^{t_1+t_2+t_3} d\tau \omega_{10}(\tau)} \rangle, \quad \text{(A1)}$$

$$R_2^{ijkl}(t_1,t_2,t_3) = R_1^{ijkl}(t_1,t_2,t_3), \quad \text{(A2)}$$

$$R_3^{ijkl}(t_1,t_2,t_3) = -\langle X_3^{ijkl}(t_1,t_2,t_3) e^{i\int_0^{t_1} d\tau \omega_{10}(\tau)} e^{-i\int_{t_1}^{t_1+t_2+t_3} d\tau \omega_{21}(\tau)} \rangle, \quad \text{(A3)}$$

$\vec{k} = \vec{k}_1 - \vec{k}_2 + \vec{k}_3$:

$$R_4^{ijkl}(t_1,t_2,t_3) = \langle X_1^{ijkl}(t_1,t_2,t_3) e^{-i\int_0^{t_1} d\tau \omega_{10}(\tau)} e^{-i\int_{t_1}^{t_1+t_2+t_3} d\tau \omega_{10}(\tau)} \rangle, \quad \text{(A4)}$$

$$R_5^{ijkl}(t_1,t_2,t_3) = R_4^{ijkl}(t_1,t_2,t_3), \quad \text{(A5)}$$

$$R_6^{ijkl}(t_1,t_2,t_3) = -\langle X_3^{ijkl}(t_1,t_2,t_3) e^{-i\int_0^{t_1} d\tau \omega_{10}(\tau)} e^{-i\int_{t_1}^{t_1+t_2+t_3} d\tau \omega_{21}(\tau)} \rangle, \quad \text{(A6)}$$

$\vec{k} = \vec{k}_1 + \vec{k}_2 - \vec{k}_3$:

$$R_7^{ijkl}(t_1,t_2,t_3) = \langle X_7^{ijkl}(t_1,t_2,t_3) e^{-i\int_0^{t_1+t_2+t_3} d\tau \omega_{10}(\tau)} e^{-i\int_{t_1}^{t_1+t_2} d\tau \omega_{21}(\tau)} \rangle, \tag{A7}$$

$$R_8^{ijkl}(t_1,t_2,t_3) = -\langle X_8^{ijkl}(t_1,t_2,t_3) e^{-i\int_0^{t_1+t_2} d\tau \omega_{10}(\tau)} e^{-i\int_{t_1}^{t_1+t_2+t_3} d\tau \omega_{21}(\tau)} \rangle, \tag{A8}$$

where

$$X_1^{ijkl}(t_1,t_2,t_3) = \mu_{10}^i(0)\mu_{10}^j(t_1)\mu_{10}^k(t_1+t_2)\mu_{10}^l(t_1+t_2+t_3), \tag{A9}$$

$$X_3^{ijkl}(t_1,t_2,t_3) = \mu_{10}^i(0)\mu_{10}^j(t_1)\mu_{21}^k(t_1+t_2)\mu_{21}^l(t_1+t_2+t_3), \tag{A10}$$

$$X_7^{ijkl}(t_1,t_2,t_3) = \mu_{10}^i(0)\mu_{21}^j(t_1)\mu_{21}^k(t_1+t_2)\mu_{10}^l(t_1+t_2+t_3), \tag{A11}$$

$$X_8^{ijkl}(t_1,t_2,t_3) = \mu_{10}^i(0)\mu_{21}^j(t_1)\mu_{10}^k(t_1+t_2)\mu_{21}^l(t_1+t_2+t_3). \tag{A12}$$

$\mu_{10}^i(t)$ is the $i$th component of the transition dipole for the 1–0 transition at time $t$ (and $\mu_{21}^i(t)$ is the same for the 2–1 transition). $\omega_{10}(t)$ is the transition frequency for the 1–0 transition at time $t$ (and $\omega_{21}(t)$ is the same for the 2–1 transition).

## APPENDIX B: DERIVATION OF EQUATION (9)

Equation (9) is derived by following the procedure developed for the response function of Raman scattering in McQuarrie's textbook.[69] First, we rewrite the components of the transition dipole in the lab-fixed $x,y,z$ frame

$$\mu_{10}^i = \sum_{\alpha=x,y,z} c_{i\alpha}\mu_{10}^\alpha, \tag{B1}$$

where $c_{i\alpha}$ is an element of the transformation matrix between the light polarization and the lab-fixed frame ($c_{ix} = \sin\theta\cos\phi$, $c_{iy} = \sin\theta\sin\phi$, $c_{iz} = \cos\theta$, where $\theta$ and $\phi$ are the polar and azimuthal angles of the polarization $\hat{i}$, respectively). Then the time-correlation function in Eq. (8) is rewritten as

$$\langle \mu_{10}^i(0)^2 \mu_{10}^k(t_2)^2 \rangle = \sum_{\alpha,\beta,\gamma,\delta} c_{i\alpha}c_{i\beta}c_{k\gamma}c_{k\delta} \langle \mu_{10}^\alpha(0)\mu_{10}^\beta(0)\mu_{10}^\gamma(t_2)\mu_{10}^\delta(t_2) \rangle. \tag{B2}$$

For isotropic systems, Eq. (B2) must be independent of the orientation of the light polarizations with respect to the lab-fixed axes. Therefore, we can equally well average over all such orientations. The spherical averages are given by[69]

$$\langle c_{i\alpha}c_{i\beta}c_{i\gamma}c_{i\delta} \rangle_{\text{sphere}} = \frac{1}{15}(\delta_{\alpha\beta}\delta_{\gamma\delta} + \delta_{\alpha\gamma}\delta_{\beta\delta} + \delta_{\alpha\delta}\delta_{\beta\gamma}), \tag{B3}$$

$$\langle c_{i\alpha}c_{i\beta}c_{k\gamma}c_{k\delta} \rangle_{\text{sphere}} = \frac{1}{30}(4\delta_{\alpha\beta}\delta_{\gamma\delta} - \delta_{\alpha\gamma}\delta_{\beta\delta} - \delta_{\alpha\delta}\delta_{\beta\gamma}), \tag{B4}$$

for $\hat{i} \perp \hat{k}$. Therefore, the time-correlation functions are given by

$$\langle \mu_{10}^i(0)^2 \mu_{10}^i(t_2)^2 \rangle = \frac{1}{15}[\langle |\vec{\mu}_{10}(0)|^2 |\vec{\mu}_{10}(t_2)|^2 \rangle + 2\langle (\vec{\mu}_{10}(0)\cdot\vec{\mu}_{10}(t_2))^2 \rangle], \tag{B5}$$

$$\langle \mu_{10}^i(0)^2 \mu_{10}^k(t_2)^2 \rangle = \frac{1}{15}[2\langle |\vec{\mu}_{10}(0)|^2 |\vec{\mu}_{10}(t_2)|^2 \rangle - \langle (\vec{\mu}_{10}(0)\cdot\vec{\mu}_{10}(t_2))^2 \rangle], \tag{B6}$$

which yield Eq. (9).


[1] *Water: A Comprehensive Treatise*, edited by F. Franks (Plenum, New York, 1972), Vol. 1.
[2] D. Wolf, *Spin-Temperature and Nuclear Spin Relaxation in Matter* (Clarendon, Oxford, 1979).
[3] J. Teixeira, M. C. Bellissent-Funnel, S. H. Chen, and A. J. Dianoux, Phys. Rev. A **31**, 1913 (1985).
[4] G. R. Fleming, *Chemical Applications of Ultrafast Spectroscopy* (Oxford University Press, New York, 1986).
[5] S. Mukamel, *Principles of Nonlinear Optical Spectroscopy* (Oxford, New York, 1995).
[6] J. L. McHale, *Molecular Spectroscopy* (Prentice Hall, New Jersey, 1999).
[7] W. W. Parson, *Modern Optical Spectroscopy* (Springer, Dordrecht, 2009).
[8] C. Rønne, L. Thrane, P.-O. Åstrand, A. Wallqvist, K. V. Mikkelsen, and S. R. Keiding, J. Chem. Phys. **107**, 5319 (1997).
[9] K. Winkler, J. Lindner, H. Bürsing, and P. Vöhringer, J. Chem. Phys. **113**, 4674 (2000).
[10] K. Krynicki, Physica (Amsterdam) **32**, 167 (1966).
[11] D. W. G. Smith and J. G. Powles, Mol. Phys. **10**, 451 (1966).
[12] B. C. Gordalla and M. D. Zeidler, Mol. Phys. **59**, 817 (1986).
[13] J. Jonas, T. DeFries, and D. J. Wilbur, J. Chem. Phys. **65**, 582 (1976).
[14] J. Ropp, C. Lawrence, T. C. Farrar, and J. L. Skinner, J. Am. Chem. Soc. **123**, 8047 (2001).
[15] I. R. Piletic, D. E. Moilanen, D. B. Spry, N. E. Levinger, and M. D. Fayer, J. Phys. Chem. A **110**, 4985 (2006).
[16] H. J. Bakker, Y. L. A. Rezus, and R. L. A. Timmer, J. Phys. Chem. A **112**, 11523 (2008).
[17] H. Bakker and J. L. Skinner, Chem. Rev. **110**, 1498 (2010).
[18] N. E. Levinger and L. A. Swafford, Annu. Rev. Phys. Chem. **60**, 385 (2009).
[19] D. E. Moilanen, E. E. Fenn, Y.-S. Lin, J. L. Skinner, B. Bagchi, and M. D. Fayer, Proc. Natl. Acad. Sci. U.S.A. **105**, 5295 (2008).
[20] L. Piatkowski, K. B. Eisenthal, and H. J. Bakker, Phys. Chem. Chem. Phys. **11**, 9033 (2009).
[21] P. A. Pieniazek, Y.-S. Lin, J. Chowdhary, B. M. Ladanyi, and J. L. Skinner, J. Phys. Chem. B **113**, 15017 (2009).
[22] Y.-S. Lin, B. M. Auer, and J. L. Skinner, J. Chem. Phys. **131**, 144511 (2009).
[23] K. J. Tielrooij, C. Petersen, Y. L. A. Rezus, and H. J. Bakker, Chem. Phys. Lett. **471**, 71 (2009).
[24] G. Lipari and A. Szabo, Biophys. J. **30**, 489 (1980).
[25] C. P. Lawrence and J. L. Skinner, J. Chem. Phys. **118**, 264 (2003).
[26] D. Laage and J. T. Hynes, Chem. Phys. Lett. **433**, 80 (2006).
[27] T. l. C. Jansen and J. Knoester, J. Phys. Chem. B **110**, 22910 (2006).
[28] T. l. C. Jansen and J. Knoester, Acc. Chem. Res. **42**, 1405 (2009).
[29] J. R. Schmidt, S. A. Corcelli, and J. L. Skinner, J. Chem. Phys. **123**, 044513 (2005).
[30] R. Kubo, Adv. Chem. Phys. **15**, 101 (1969).
[31] H. J. Bakker, Chem. Rev. **108**, 1456 (2008).

[32] M. D. Fayer, D. E. Moilanen, D. Wong, D. E. Rosenfeld, E. E. Fenn, and S. Park, Acc. Chem. Res. **42**, 1210 (2009).
[33] E. E. Fenn, D. E. Moilanen, N. E. Levinger, and M. D. Fayer, J. Am. Chem. Soc. **131**, 5530 (2009).
[34] A. M. Dokter, S. Woutersen, and H. J. Bakker, Phys. Rev. Lett. **94**, 178301 (2005).
[35] A. M. Dokter, S. Woutersen, and H. J. Bakker, Proc. Natl. Acad. Sci. U.S.A. **103**, 15355 (2006).
[36] D. E. Moilanen, E. E. Fenn, D. Wong, and M. D. Fayer, J. Phys. Chem. B **113**, 8560 (2009).
[37] D. E. Moilanen, E. E. Fenn, D. Wong, and M. D. Fayer, J. Chem. Phys. **131**, 014704 (2009).
[38] D. E. Moilanen, E. E. Fenn, D. Wong, and M. D. Fayer, J. Am. Chem. Soc. **131**, 8318 (2009).
[39] G. M. Gale, G. Gallot, and N. Lascoux, Chem. Phys. Lett. **311**, 123 (1999).
[40] D. Laage and J. T. Hynes, Proc. Natl. Acad. Sci. U.S.A. **104**, 11167 (2007).
[41] A. Paarmann, T. Hayashi, S. Mukamel, and R. J. D. Miller, J. Chem. Phys. **130**, 204110 (2009).
[42] J. G. Saven and J. L. Skinner, J. Chem. Phys. **99**, 4391 (1993).
[43] M. D. Stephens, J. G. Saven, and J. L. Skinner, J. Chem. Phys. **106**, 2129 (1997).
[44] J. R. Schmidt, N. Sundlass, and J. L. Skinner, Chem. Phys. Lett. **378**, 559 (2003).
[45] B. Auer and J. L. Skinner, J. Chem. Phys. **127**, 104105 (2007).
[46] J. L. Skinner, B. M. Auer, and Y.-S. Lin, Adv. Chem. Phys. **142**, 59 (2009).
[47] K. Hermansson, S. Knuts, and J. Lindgren, J. Chem. Phys. **95**, 7486 (1991).
[48] R. Rey, K. B. Møller, and J. T. Hynes, J. Phys. Chem. A **106**, 11993 (2002).
[49] K. B. Møller, R. Rey, and J. T. Hynes, J. Phys. Chem. A **108**, 1275 (2004).
[50] C. P. Lawrence and J. L. Skinner, J. Chem. Phys. **117**, 8847 (2002).
[51] C. P. Lawrence and J. L. Skinner, Chem. Phys. Lett. **369**, 472 (2003).
[52] S. A. Corcelli, C. P. Lawrence, and J. L. Skinner, J. Chem. Phys. **120**, 8107 (2004).
[53] S. A. Corcelli and J. L. Skinner, J. Phys. Chem. A **109**, 6154 (2005).
[54] B. Auer, R. Kumar, J. R. Schmidt, and J. L. Skinner, Proc. Natl. Acad. Sci. U.S.A. **104**, 14215 (2007).
[55] T. Hayashi, T. l. C. Jansen, W. Zhuang, and S. Mukamel, J. Phys. Chem. A **109**, 64 (2005).
[56] J. D. Smith, C. D. Cappa, K. R. Wilson, R. C. Cohen, P. L. Geissler, and R. J. Saykally, Proc. Natl. Acad. Sci. U.S.A. **102**, 14171 (2005).
[57] E. Harder, J. D. Eaves, A. Tokmakoff, and B. J. Berne, Proc. Natl. Acad. Sci. U.S.A. **102**, 11611 (2005).
[58] J. B. Asbury, T. Steinel, C. Stromberg, S. A. Corcelli, C. P. Lawrence, J. L. Skinner, and M. D. Fayer, J. Phys. Chem. A **108**, 1107 (2004).
[59] S. A. Corcelli, C. P. Lawrence, J. B. Asbury, T. Steinel, M. D. Fayer, and J. L. Skinner, J. Chem. Phys. **121**, 8897 (2004).
[60] J. R. Schmidt, S. A. Corcelli, and J. L. Skinner, J. Chem. Phys. **121**, 8887 (2004).
[61] J. R. Schmidt, S. T. Roberts, J. J. Loparo, A. Tokmakoff, M. D. Fayer, and J. L. Skinner, Chem. Phys. **341**, 143 (2007).
[62] H. J. C. Berendsen, J. R. Grigera, and T. P. Straatsma, J. Phys. Chem. **91**, 6269 (1987).
[63] D. van der Spoel, E. Lindahl, B. Hess, A. R. van Buuren, E. Apol, P. J. Meulenhoff, D. P. Tieleman, A. L. T. M. Sijbers, K. A. Feenstra, R. van Drunen, and H. J. C. Berendsen, *Gromacs User Manual Version 3.3*, www.gromacs.org (2005).
[64] H. Bekker, H. J. C. Berendsen, E. J. Dijkstra, S. Achterop, R. van Drunen, D. van der Spoel, A. Sijbers, H. Keegstra, B. Reitsma, and M. K. R. Renardus, *Physics Computing 92*, edited by R. A. Groot and J. Nadrchal (World Scientific, Singapore, 1993).
[65] H. J. C. Berendsen, D. van der Spoel, and R. van Drunen, ChemPhysChem **91**, 43 (1995).
[66] E. Lindahl, B. Hess, and D. van der Spoel, J. Mol. Model. **7**, 306 (2001).
[67] D. Van Der Spoel, E. Lindahl, B. Hess, G. Groenhof, A. E. Mark, and H. J. C. Berendsen, J. Comput. Chem. **26**, 1701 (2005).
[68] L. Piatkowski, personal communication (January 2010).
[69] D. A. McQuarrie, *Statistical Mechanics* (Harper and Row, New York, 1976).